Journal of Applied Sciences

ISSN 1812-5654

science alert

ANSInet
an open access publisher
http://ansinet.com

Journal of Applied Sciences 9 (23): 4115-4126, 2009
ISSN 1812-5654

Neotectonics of the South Central Alborz Drainage Basin, in NW Tehran, N Iran

[1]R. Khavari, [2]M. Arian and [3]M. Ghorashi
[1]Islamic Azad University, Behbahan Branch, Behbahan, Iran
[2]Islamic Azad University, Sciences and Research Branch, Hesarak, Punak Square, Tehran, Iran
[3]Geological Survey of Iran, Meraj Street, Azadi Square, Tehran, Iran

Abstract: The study records evidences of neotectonic activities in the South flank of the Central Alborz mountain range that found to be responsible for the present-day geomorphic set-up of the area since the last phase of major uplifting. Geomorphic indices indicate the presence of differential uplifting in the geological past. Neotectonic activity of the study area is investigated by a large number of geomorphic indices of DEM-derived catchments and drainage lines using GIS: drainage basin asymmetry, stream gradient, channel width and depth as well as sinuosity. The stream network asymmetry was studied using morphometric measures of transverse topographic symmetry, asymmetry factor and drainage basin shape. Analysis of the drainage basin and a number of subcatchments in the study area results in a field of T-vectors that defines anomalous zones of the basin asymmetry. This method demonstrates a neotectonic tilting of the drainage basin toward W-NW. Subcatchments of the basin indicate different directions of stream migration depending on their flow direction in the area. There are neither lithologic controls nor localized climate that causes the asymmetry, so it seems reasonable for the stream migration that tectonics can account.

Key words: Neotectonics, asymmetry, basin shape, bed rock river, GIS

INTRODUCTION

Surrounding the south Caspian Basin, the narrow Alborz mountain of 100 km wide extends for about 2000 km from Lesser Caucasus in the Northwest to the Paropamisus mountains in Northern Afghanistan, to the East (Fig. 1a) and shows strong tectonic activity (Berberian and Yeats, 2001). A V-shaped structure characterizes the central part of Alborz with folds and faults trending NW-SE in the Western side and trending NE-SW in the Eastern (Ritz *et al*., 2006). Although, there are many studies on DEM-derived catchments and drainage lines (Reinfelds *et al*., 2004; Hayakawa and Oguchi, 2006; Barry *et al*., 2007) and tectonic control upon forms of rivers and streams in recent years (Alexander and Leeder, 1990; Schumm *et al*., 2000; Burbank and Anderson, 2001; Keller and Pinter, 2002; Salvany, 2004; El-Hamdouni *et al*., 2008), little attention has been paid to active tectonics and rivers in the Alborz mountain range (Allen *et al*., 2003; Nazari *et al*., 2009). Present-day geomorphology of the South flank of the Central Alborz mountain range is the result of active tectonic processes. On the basis of geomorphic indices, we have attempted to work out the geomorphological evolution. The recent investigations show that neotectonism has played a key role in the geomorphic evolution of this part of the Alborz mountain range. In this study, the values of tectonic activity are determined based on the tilting magnitude in different part of the Karaj River drainage basin, one of the most important rivers in N Iran.

MATERIALS AND METHODS

Drainage pattern recognized from DEM: Using the hydrologic modeling functions in ArcGIS (Arc hydro tools), it is possible to obtain the direction of surface water flow, the drainage area and stream networks from the filled DEM. A Digital Elevation Model (DEM) is used to determine which cells flow into other cells (the flow direction). However, if there are errors in the digital elevation model, using hydrologic analysis functions, it is possible to identify them and fill. The flow direction can obtain from this depressionless elevation model. To delineating watersheds, it's necessary to identify pour points; these locations can be the mouths of streams at which water flows out of an area. Once the direction of flow out of each cell is known, it is possible to determine which and how many cells flow into any given cell. This information can be used to define watershed boundaries and stream networks. Stream heads are almost consistent with the beginning of blue lines of streams on the topographic maps that used to derive DEM.

Corresponding Author: R. Khavari, Islamic Azad University, Behbahan Branch, Behbahan, Iran
Tel: +00989374105028 Fax: +98671-4220109

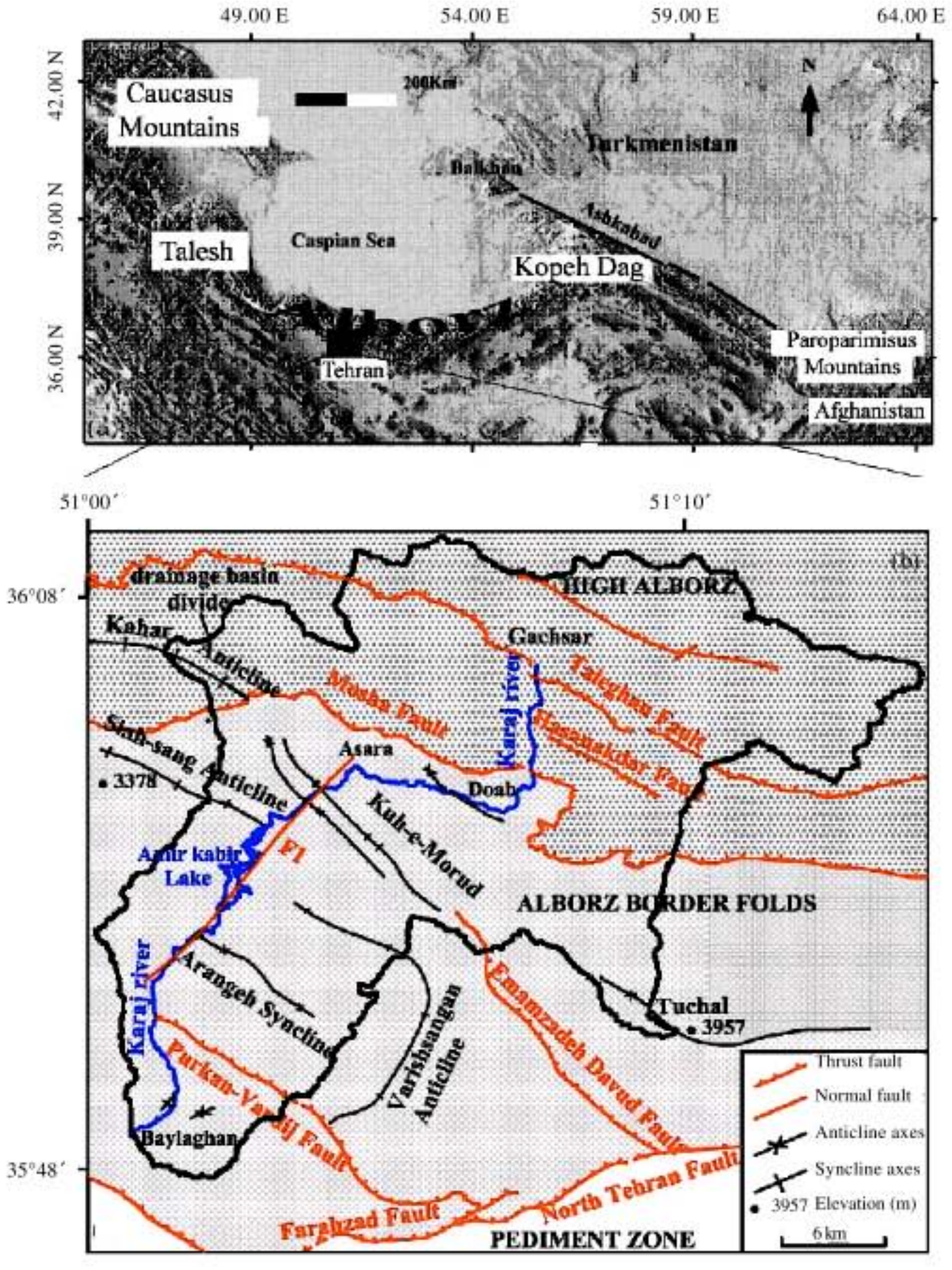

Fig. 1: Location and geological setting of the study area, (a) summary map of the Alborz Range (modified from Ehteshami and Yassaghi, 2006) and (b) spatial relations of major structural elements and the Karaj drainage basin, N Iran. The main faults and fold axises that affected flow direction of the Karaj River and other drainage lines are shown (modified from Gansser and Hubber, 1962)

In this study, we have used 10 m grid cell DEM. Its projection was the UTM zone 39 N. The DEM was derived from the contour lines of the 1: 25,000 topographic maps with 10 m contour intervals. This study took 18 months from June 2007 to December 2008 and its final report was provided in April 2009.

Transverse topographic symmetry factor (T): The transverse topographic symmetry factor (T) is a method that evaluates the amount of asymmetry of a river within a basin and the variation of this asymmetry in different segments of valley. The basin midline would be the location of a river that is symmetrically placed with regard to the basin divide. It is calculated regarding the larger axis of the basin, which extends from the outlet of the basin to the most distal point in the headwater (Fig. 10). For each segment, T is the ratio of the distance from the basin midline to the active meander-belt midline (D_a) and to the basin divide (D_d):

$$T = D_a/D_d \quad (1)$$

This value varies between 0 and 1, which represent the minimum and maximum asymmetry of a segment,

respectively. It can be represented as a two-dimensional vector with a length equivalent to D_d/D_d and a direction perpendicular to the segment that indicates movement of the segment (as well as the river) with regard to the basin midline (Salvany, 2004). As suggested by Cox (1994), the most probable tilt direction is that indicated by the mean vector magnitude obtained from the measurement of basin segments, thus allowing discrimination between preferred stream migration as a consequence of internal fluvial processes or as a consequence of external forces.

Asymmetric Factor (AF): The Asymmetric Factor (AF) is a way to evaluate the existence of tectonic tilting at the scale of drainage basin. It is defined as:

$$AF = 100\ (A_r/A_t) \quad (2)$$

where, A_r is the area of the basin to the right of the trunk stream and A_t is the total area of the drainage basin.

When AF = 50, the drainage basin is perfectly symmetric, while values greater or less than 50 belong to asymmetric basins. This method may be applied over a relatively large area (Keller and Pinter, 2002).

Drainage basin shape (B_s): Relatively young drainage basins in active tectonic areas tend to be elongated in shape normal to the topographic slope of mountain. With continued evolution or less active tectonic processes, the elongated shape tends to evolve to a more circular shape (Bull and McFadden, 1977). Horizontal projection of basin shape may be described by the elongation ratio, B_s (Ramírez-Herrera, 1998) expressed by equation

$$B_s = B_l/B_w \quad (3)$$

where B_l is the length of the basin, measured from its outlet to the most distal point in the drainage divide and B_w is the width of the basin measured across the short axis.

The index reflects differences between elongated basins with high values of B_s and more circular basins with low values. Basins with elongated shapes are characteristic of tectonically active areas, where the stream was primarily downcutting. Rapidly uplifted mountain fronts generally produce elongated, steep basins; and when tectonic activity is diminished or ceases, widening of the basins occur from the mountain front up (Ramírez-Herrera, 1998).

Ratio of valley floor width to valley height (V_f): The V_f is defined as the ratio of the width of the valley floor to its average height (Bull and McFadden, 1977) and is computed by:

$$V_f = 2V_{fw}/[(E_{ld} - E_{sc})] + (E_{rd} - E_{sc})] \quad (4)$$

where, V_f is the ratio of valley floor width to valley height, V_{fw} is the width of the valley floor, E_{ld} is the elevation of the divide on the left side of the valley, E_{rd} is the elevation on the right side and E_{sc} is the average elevation of the valley floor.

This index differentiates between valleys with a wide floor relative to the height of valley walls with a U-shape compared to narrow, steep valleys with a V-shape. Valleys with a U-shape generally have high values of V_f, whereas V-shaped valleys with relatively low values. Because uplift is associated with incision, the index is thought to be a surrogate for active tectonics where low values of V_f are associated with higher rates of uplift and incision. The index is a measure of incision and not uplift; but in an equilibrium state, incision and uplift are nearly matched. Calculation of the index is done at a prescribed distance upstream from the mountain front (Silva *et al*., 2003).

STUDY AREA

The Karaj drainage basin of the South Central Alborz has an area of about 1085 km and a length and width, 59 and 37 km, respectively. The Karaj River with 67 km long originates in the Southern part of the Central Alborz at 2200 m sea level, flowing southward to Amirkabir lake and finally debouches on to the Karaj alluvial fan close to 1360 m over sea level (Fig. 1b). The topography contrast is a little pronounced in the study area; the highest peak of the drainage divide is about 4400 m in elevation, drops to 1300 m in the outlet of the basin (Fig. 7).

Study area extends over two units of the Alborz subdivision (Fig. 1b); the high Alborz, a complex folded zone of Precambrian, Paleozoic and Mesozoic sedimentary rocks thrust southwards over Eocene rocks in the border folds zone, forms the hanging-wall of the Mosha fault (Ehteshami and Yassaghi, 2006) and the Border Folds zone contains the Eocene Karaj formation which crops out in a series of synclines in the footwall of fault (Fig. 1-3 and 6). The Palaeocene Fajan continental conglomerates throughout northern Iran marks the base of the Eocene Karaj formation (Fig. 3-5) (Ehteshami and Yassaghi, 2006). Dedual (1967), has distinguished the five members in the Karaj valley: (1) Kandavan shale, (2) Upper tuff member, (3) Asara shale, (4) Middle tuff member and (5) Lower shale member (Fig. 2). The North Tehran fault upthrusts the rocks of the Karaj formation southwards over the alluvial deposits of the Pediment zone (Fig. 1). Alluvial deposits are rare in the Karaj River valley, so, it flows over a channel of exposed bedrock

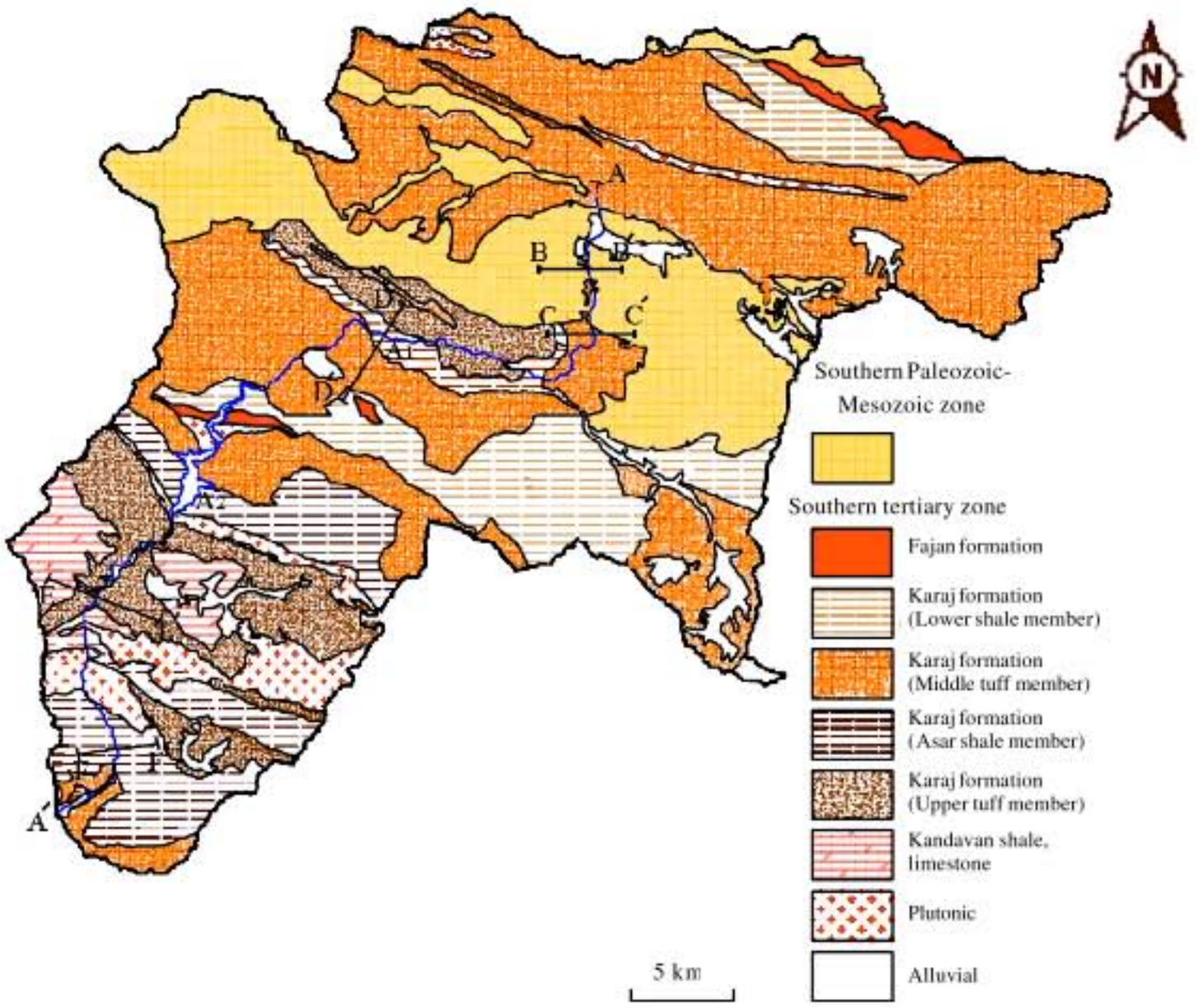

Fig. 2: Map of the Karaj drainage basin showing the bedrock lithology (modified from Emami, 1993; Vahdati-Daneshmand, 2001)

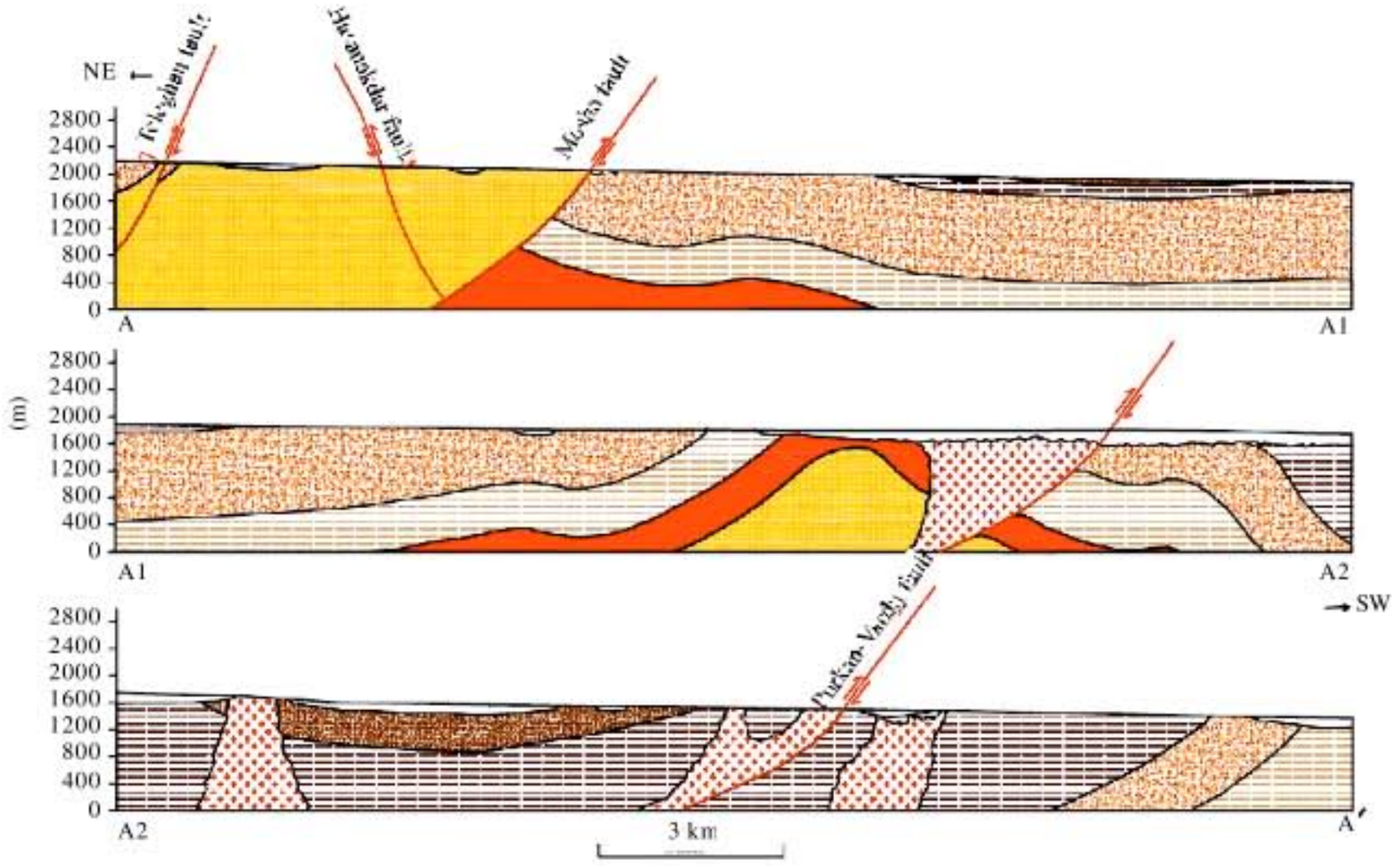

Fig. 3: Geological cross-section along the Karaj River (Fig. 2 for location and legend)

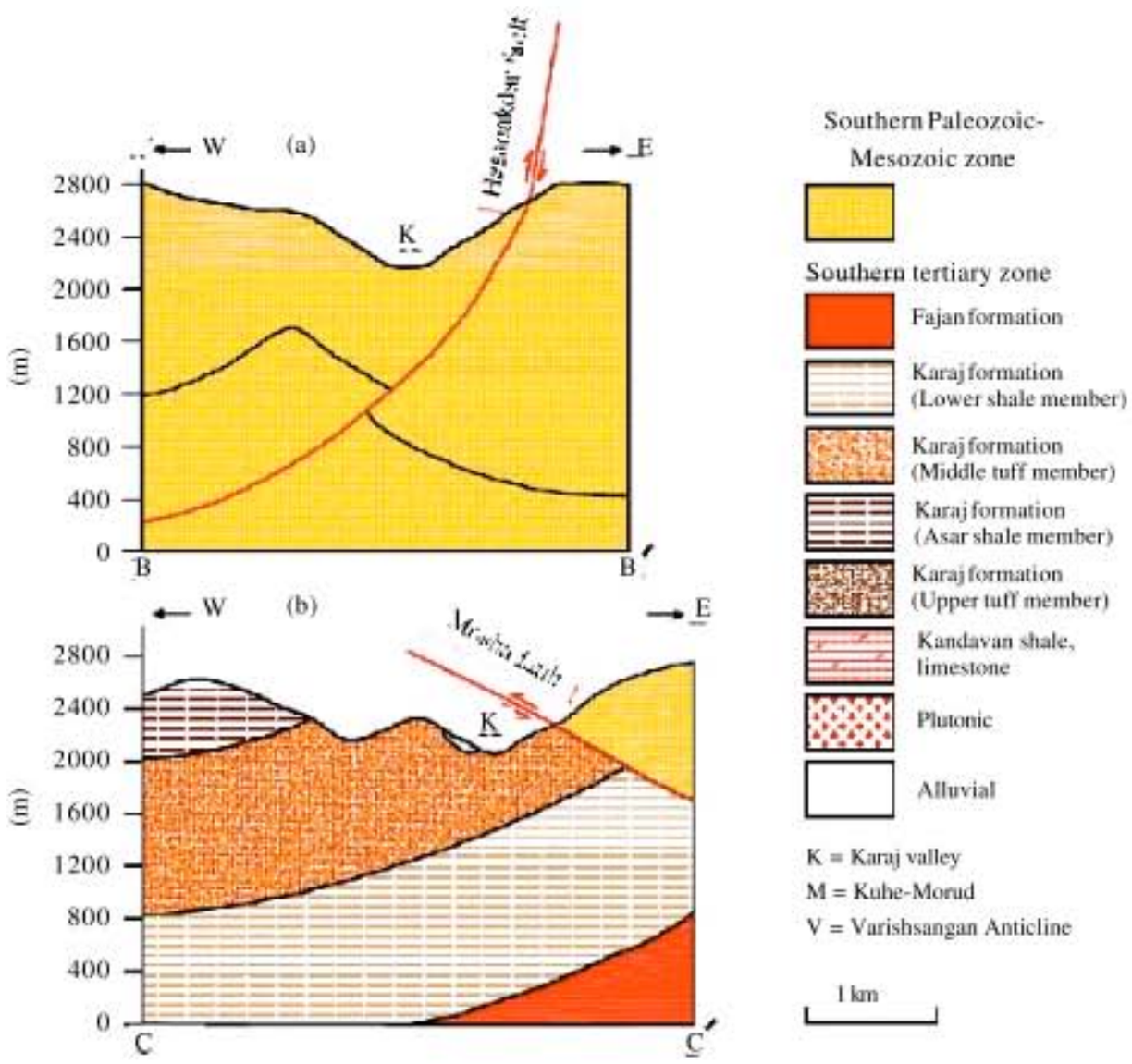

Fig. 4: Geological cross-sections across the Karaj River in upstream (Fig. 2 for locations)

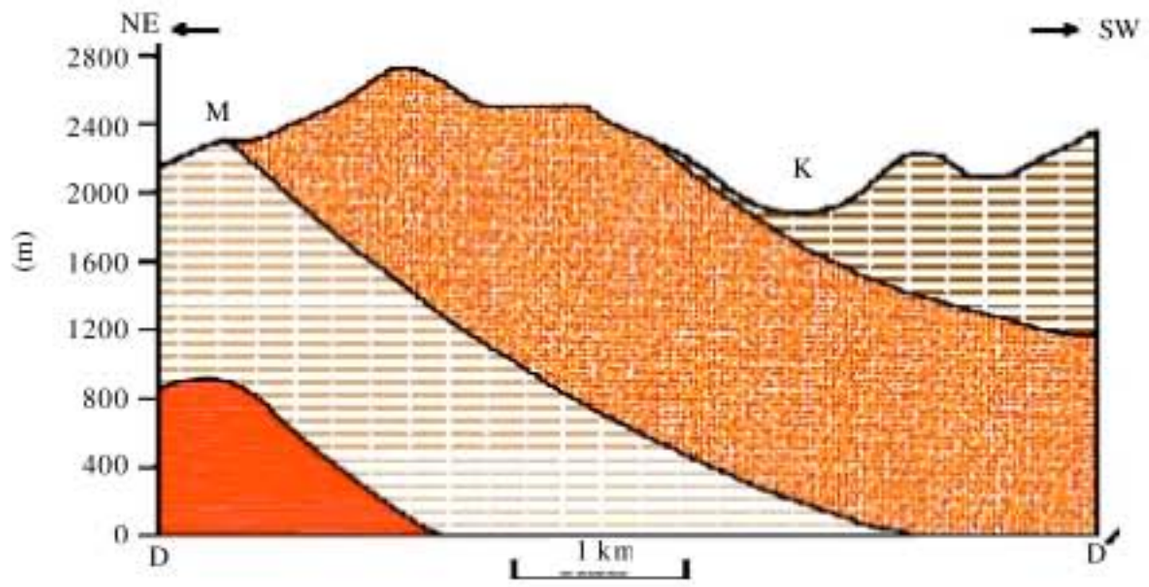

Fig. 5: Geological cross-section across the Karaj River in it's central portion (Fig. 2 for location and lithology)

over much of its length (Fig. 3). Figure 3 shows that the Karaj River is a bed rock river in that driving forces tend to be greater than resisting forces and most of deposits supplied transport away.

Significant changes of slope are rare along the Karaj River and always related to changes in the lithology. This feature is specially shown by the Karaj longitudinal profile (Fig. 8). It clearly displays 3 sections: the 1st section is an upper area where the river flows over Paleozoic-Mesozoic sedimentary rocks with a slope average of 1%, the 2nd section, downstream of the Amirkabir dam, where the river flows over Tertiary hard plutonic rocks and has the maximum slope value and the 3rd section, where the river flows over soft Tertiary rocks and has the slope average of 0.8%. There are rapid slope changes between each section, especially between the second and third sections, where there is a step with up to 11% slope. These values are consistent with the SL (Stream Length-gradient index) values for each segment along the Karaj River (Fig. 8).

The climate of the study area is cold and semi humid with an average temperature varying from -20 to 42°C and relative humidity from 38 to 72%. The annual mean

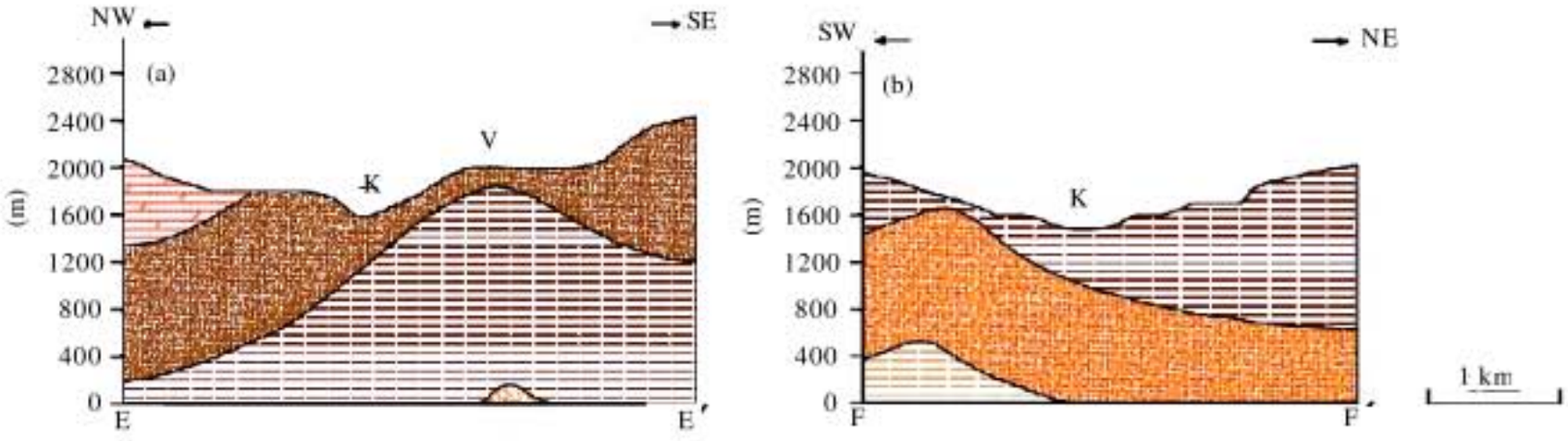

Fig. 6: Geological cross-sections across the Karaj River in downstream (Fig. 2 for locations and lithology)

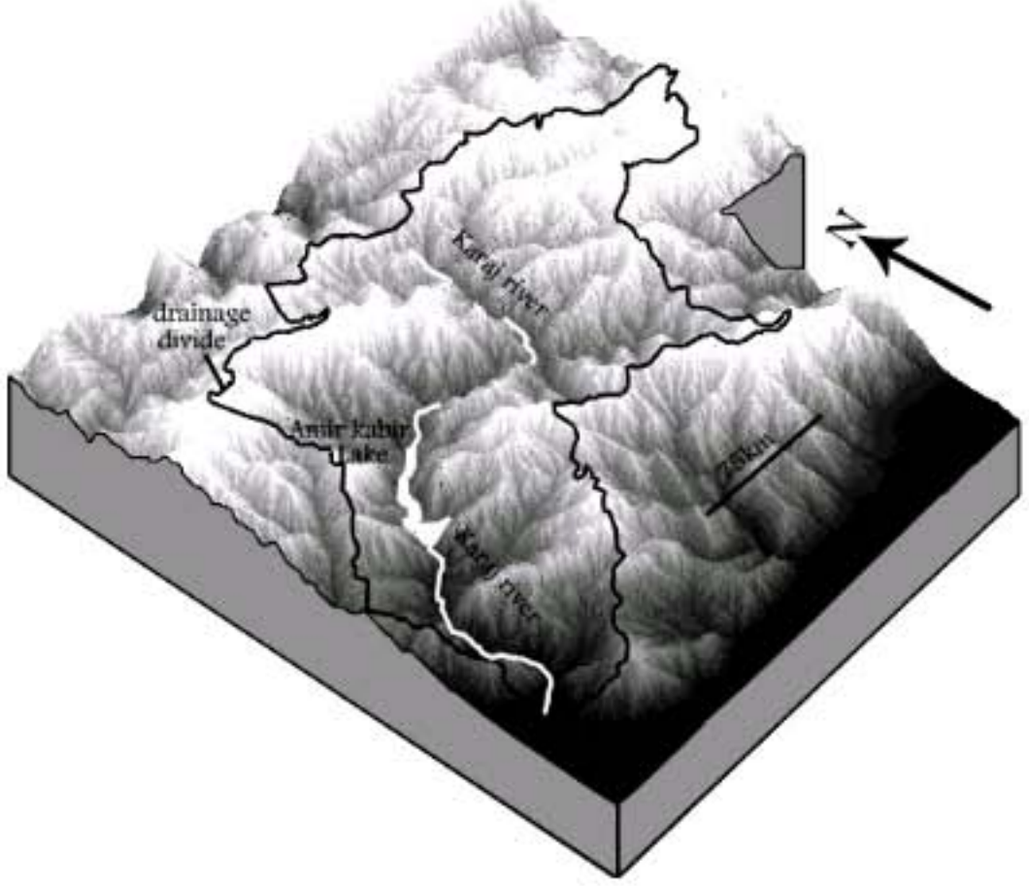

Fig. 7: Digital elevation model of the Karaj drainage basin

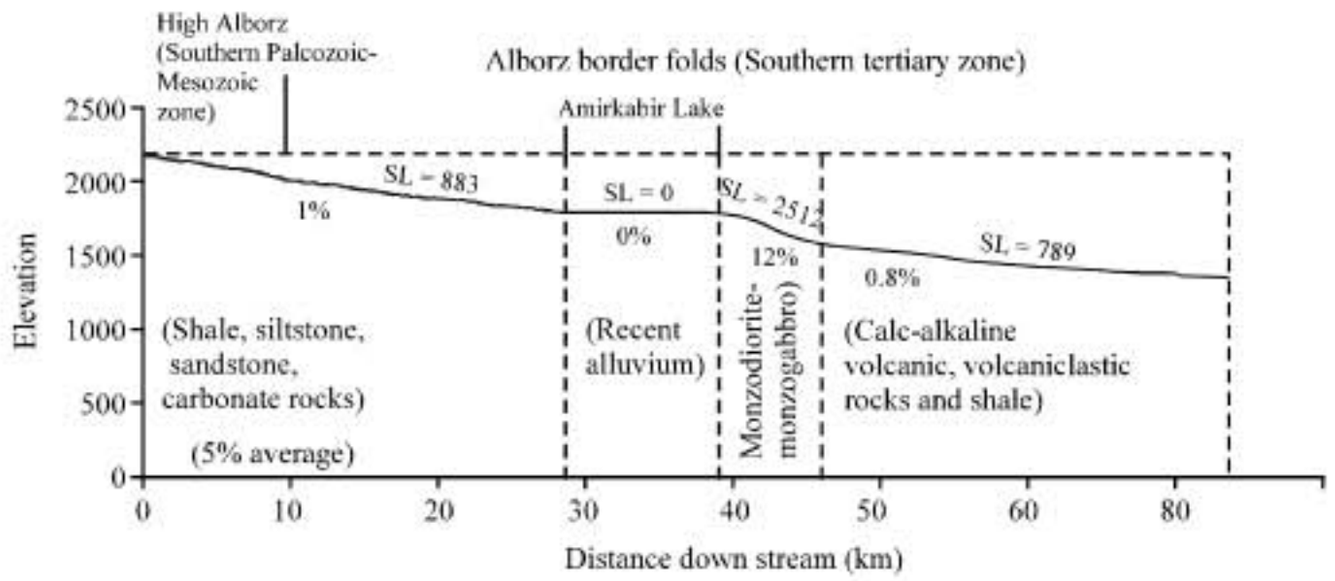

Fig. 8: Longitudinal river profile of the Karaj River, derived from 10 m DEM, showing the relationship between the slope and the bedrock lithology, SL index values are indicated

precipitation is about 251 mm and maximum and minimum of the precipitation occur in winter and summer, respectively. Study area is significantly covered with herbal plant and plantation crops.

RESULTS AND DISCUSSION

In the study are 94 subcatchments were extracted from DEM (Fig. 9). The transverse topographic symmetric

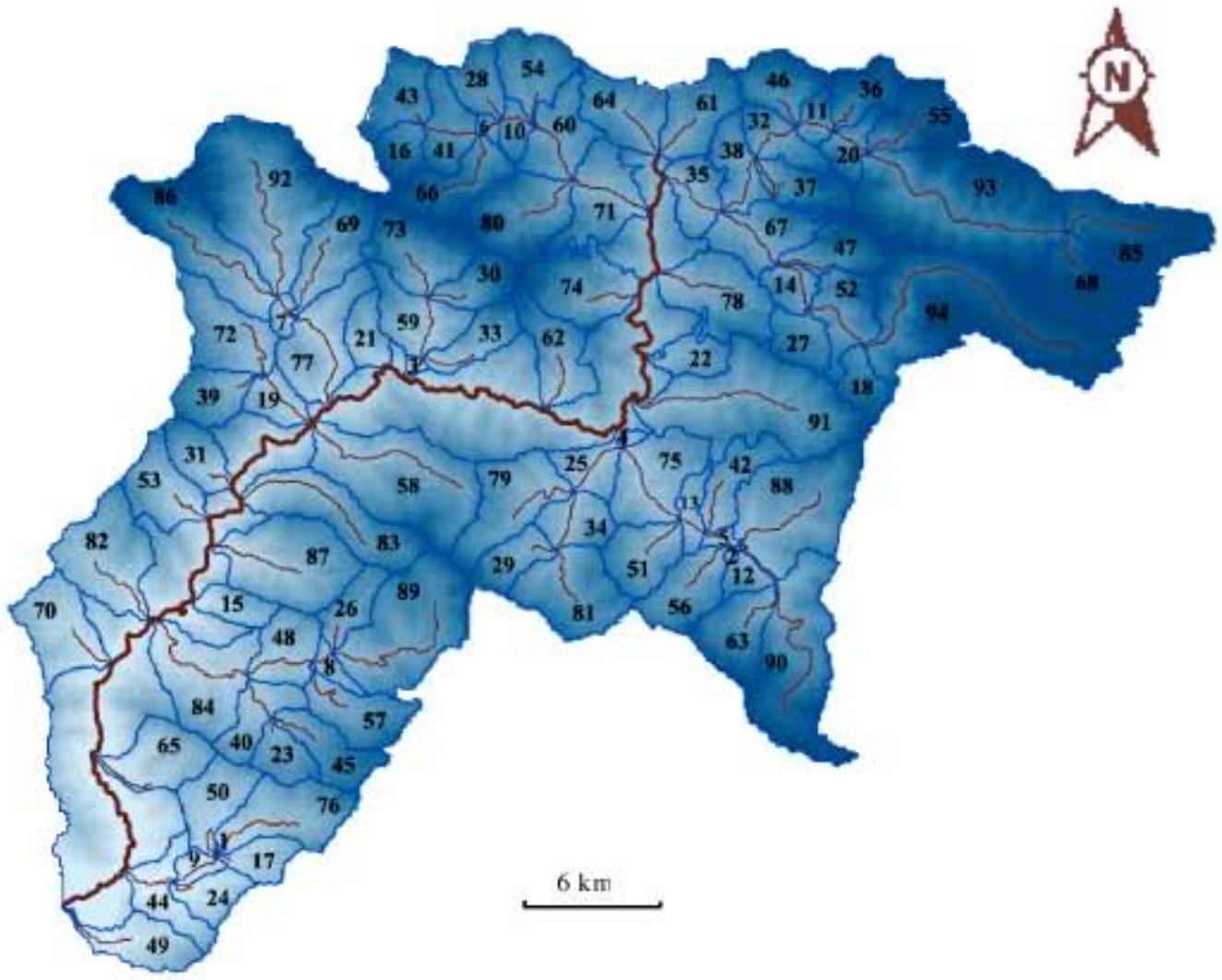

Fig. 9: DEM-derived subcatchments and drainage lines of the Karaj drainage basin

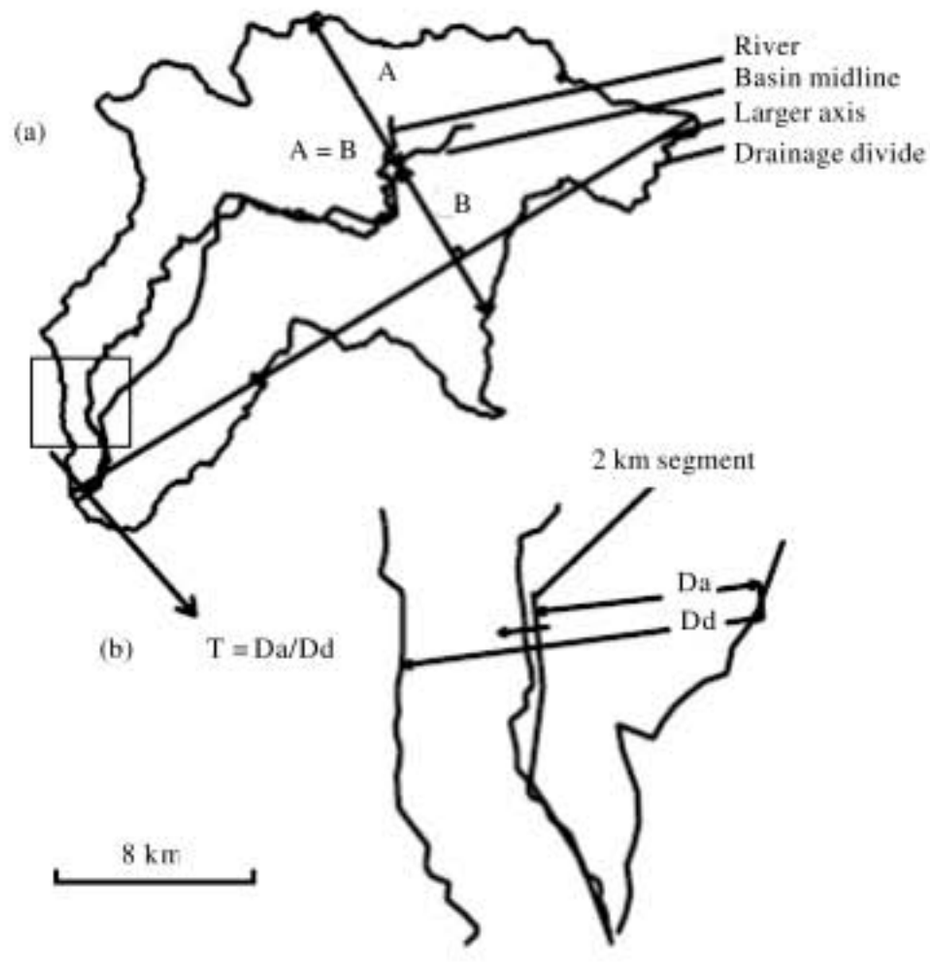

Fig. 10: Transverse topographic symmetry method after Cox (1994)

factor method applied to the Karaj drainage basin is shown in Fig. 10. We divided drainage lines into segments of the same length (2 km in this case). So, drainage lines shorter than 2 km were excluded, because their lengths were close to or smaller than 2 km segments (Table 1). Basin asymmetry vectors and their frequency diagram for the Karaj River and its tributaries are shown in Fig. 11 and 12, respectively (length of vector denotes tilting magnitude). The mean vector magnitude was obtained from the measurement of basin segments and shown

Table 1: Characteristics of drainage basins with geomorphic indices

					Stream long profile				Transverse topographic	
Basin	River length (km)	Surface area (km^2)	Sinuosity	V_f	Range of slope (%)	Average slope (%)	AF	BS	T	Bearing
Karaj	87.55	1084.600	2.20	0.39	0.2	242	34	3.18	0.2	242
1	0.30	0.088	1.56	2.08	—	—	79	4.97	—	—
2	0.50	0.43	1.18	0.38	—	—	19	1.13	—	—
3	1.22	0.70	1.08	0.62	—	—	58	1.84	—	—
4	0.84	0.83	1.05	0.21	—	—	80	2.19	—	—
5	1.57	1.08	1.27	1.90	—	—	50	2.33	—	—
6	1.26	1.08	1.09	0.88	—	—	46	1.44	—	—
7	1.45	1.72	1.13	0.81	—	—	72	1.00	—	—
8	1.06	2.16	1.12	0.13	—	—	24	3.82	—	—
9	2.49	2.27	1.20	0.15	4- 42	23	60	2.71	0.34	146
10	1.84	2.86	1.20	0.18	—	—	73	1.23	—	—
11	1.96	2.94	1.18	0.15	—	—	63	2.09	—	—
12	2.33	3.03	1.08	0.24	0.2-21	10.5	6	2.02	0.96	47
13	1.39	3.48	1.09	0.55	—	—	69	2.09		
14	2.90	4.07	1.25	0.21	1-27	14	25	1.59	0.28	72
15	0.15	4.55	1.04	0.25	—	—	58	3.45	—	—
16	0.06	4.72	1.00	0.13	—	—	38	2.02	—	—
17	0.67	4.75	1.06	0.57	—	—	33	3.08	—	—
18	0.10	4.80	1.00	0.35	—	—	37	2.59	—	—
19	3.20	4.80	1.07	0.06	1.2-17	8.9	67	2.18	0.44	48
20	1.88	4.94	1.09	0.17	—	—	36	1.43	—	—
21	0.26	5.023	1.23	0.32	—	—	45	2.44	—	—
22	1.11	5.19	1.20	0.32	—	—	48	2.78	—	—
23	0.70	5.27	1.11	0.45	—	—	19	2.31	—	—
24	1.19	5.28	1.35	0.20	—	—	20	2.64	—	—
25	3.30	5.41	1.11	0.15	5-12.2	8.7	47	2.07	0.38	319
26	1.41	5.63	1.13	0.16	—	—	57	3.53	—	—
27	0.46	5.80	1.10	0.40	—	—	14	1.63	—	—
28	1.26	6.01	1.13	0.92	—	—	65	2.22	—	—
29	1.34	6.34	1.25	0.22	—	—	48	2.85	—	—
30	1.88	6.36	1.12	0.16	—	—	46	2.91	—	—
31	1.43	6.48	1.21	0.10	—	—	48	2.64	—	—
32	2.73	6.47	1.30	0.26	9.2-22.4	15.8	46	1.83	0.08	345
33	2.54	6.54	1.12	0.10	15.9-49	32.4	63	3.68	0.02	187
34	2.76	6.55	1.07	0.13	0.8-16	8.4	64	1.12	0.39	289
35	3.50	6.75	1.20	0.15	8.3-23.5	15.9	58	1.44	0.05	17
36	2.04	6.91	1.30	0.20	12.6-40	26.3	49	2.48	0.19	128
37	2.08	6.96	1.22	0.47	2.8-52.5	27.6	50	3.67	0.44	238
38	3.45	6.97	1.24	0.31	0.4-20	10	76	3.07	0.24	111
39	2.00	7.03	1.15	0.14	—	—	50	2.68	—	—
40	2.50	7.10	1.15	2.23	7.3-22.2	14.8	38	2.24	0.37	233
41	2.90	7.60	1.13	0.27	0.6-29	14.8	45	1.94	0.09	192
42	3.03	7.70	1.29	0.16	6-32.6	19.3	51	3.44	0.38	287
43	0.62	7.75	1.09	0.87	—	—	65	1.75	—	—
44	2.80	7.85	1.29	0.03	5.4-7.4	6.4	34	3.40	0.25	328
45	2.46	7.86	1.18	0.07	10.1-20.3	15.2	66	3.70	0.38	203
46	1.73	8.05	1.17	0.44	—	—	31	1.67	—	—
47	3.06	8.09	1.19	0.28	3.2-37.3	20.3	72	3.28	0.78	180
48	3.54	8.15	1.23	0.54	3.4-18	10.7	71	2.00	0.25	336
49	4.20	8.38	1.25	0.41	2.5-12	7.3	41	5.20	0.06	197
50	1.57	8.075	1.26	0.24	—	—	83	2.40	—	—
51	2.38	8.82	1.12	0.13	0.5-35.4	18	44	1.93	0.001	312
52	3.72	9.05	1.23	0.14	11-26.3	18.7	68	1.52	0.13	230
53	2.11	9.21	1.11	0.07	7.6-55.5	31.6	66	2.40	0.3	34
54	1.65	9.27	1.10	0.89	—	—	60	2.18	—	—
55	3.53	9.40	1.25	0.24	6.4-32.5	19.5	60	2.32	0.45	131
56	3.02	9.44	1.19	0.12	1.5-52	26.8	48	2.64	0.28	311
57	3.23	9.49	1.27	0.04	3.4-25	14.2	27	2.56	0.55	61
58	13.59	25.69	1.89	0.09	3.3-18.42	10.7	41	2.79	0.41	24
59	3.13	9.64	1.15	0.15	2.2-26.4	14.3	65	2.54	0.44	94
60	2.24	9.65	1.13	0.94	0.7-30	15.4	35	2.34	0.39	64
61	2.44	9.81	1.09	0.16	14.2-40	27.2	38	2.51	0.33	317
62	3.15	9.97	1.24	0.46	7.9-16.4	12.2	46	3.36	0.39	275
63	3.01	10.12	1.28	0.05	2-32.9	17.5	48	2.40	0.41	130

Table 1: Continued

Basin	River length (km)	Surface area (km^2)	Sinuosity	V_f	Stream long profile: Range of slope (%)	Stream long profile: Average slope (%)	AF	BS	Transverse topographic: T	Transverse topographic: Bearing
64	2.58	10.19	1.06	0.13	14.8-32	23.40	45	2.70	0.40	227
65	3.29	10.31	1.18	1.55	6.2-23.2	14.70	75	2.90	0.65	205
66	4.14	10.35	1.35	0.26	3.5-39.6	21.50	66	2.46	0.26	312
67	3.83	10.47	1.13	0.16	2.4-13	7.80	59	2.55	0.035	48
68	2.07	10.76	1.27	0.87	3.9-42	22.80	31	2.10	0.590	70
69	4.93	11.15	1.17	0.16	5.3-12.5	8.90	37	3.67	0.20	203
70	2.71	11.76	1.17	0.12	3.5-50.6	27.10	54	2.27	0.31	51
71	4.37	11.80	1.17	0.40	1.1-27.8	14.40	58	2.10	0.29	113
72	3.06	11.93	1.25	1.01	7.7-29	18.30	70	3.01	0.27	60
73	2.55	12.87	1.16	0.04	13.8-22.2	18.00	23	1.88	0.43	237
74	2.71	13.07	1.14	0.18	1.1-31.7	16.40	48	2.22	0.21	169
75	4.51	13.12	1.12	0.13	8-14.2	11.11	61	1.22	0.30	141
76	4.74	13.26	1.26	0.22	3.7-27.8	15.70	66	3.40	0.35	166
77	5.23	13.55	1.26	0.63	0.78-17.2	9.00	49	3.21	0.26	159
78	3.89	13.76	1.13	0.17	5.4-23.9	14.60	58	2.57	0.32	104
79	3.58	13.87	1.24	0.20	2.02-33.2	17.60	27	2.80	0.56	64
80	3.61	14.06	1.24	0.12	0.7-31	15.90	65	2.11	0.16	326
81	3.02	14.09	1.22	0.05	7.6-34.5	21.10	42	1.24	0.40	247
82	4.32	15.64	1.21	0.20	9.8-12.4	11.10	50	2.51	0.27	57
83	7.69	15.77	1.32	0.05	9-21	15.00	43	4.56	0.20	151
84	7.30	15.89	1.52	0.32	3.5-51.2	27.30	35	2.29	0.30	38
85	4.93	17.46	1.24	0.08	3.5-23.8	13.60	40	2.47	0.31	12
86	7.34	18.29	1.24	0.11	5.7-31.8	18.70	50	4.00	0.36	97
87	4.65	19.06	1.11	0.10	0.5-33.9	17.20	48	2.44	0.24	108
88	5.95	21.75	1.35	0.24	1-24.6	13.00	50	2.47	0.085	242
89	7.40	22.79	1.46	0.22	4-12.8	8.40	50	2.10	0.32	90
90	9.10	23.95	1.60	0.30	2.6-31.7	17.15	53	3.04	0.31	145
91	8.53	30.85	1.20	0.15	5.1-6.3	5.70	45	3.46	0.30	270
92	7.94	30.97	1.28	0.54	4.5-8.8	6.60	43	2.18	0.07	168
93	11.44	39.33	1.21	0.23	4.5-10.4	7.50	49	2.25	0.30	77
94	14.09	40.39	1.50	0.17	2.9-11.5	7.20	41	3.68	0.32	127

in Fig. 13. Mean vector magnitude for the Karaj River and its tributaries was 0.07 (T-values), 359° (bearing). Mean vector magnitude for the Karaj River and its tributaries parallel to the structures was 0.1 (T-values), 39° (bearing), while in the North and South parts of the Karaj River and tributaries parallel to these parts, mean vector was 0.1 (T-values), 288° (bearing). The values of AF, B_s and V_f were calculated for all of the subcatchments (Table 1). The maximum values of AF are obtained in subcatchments 1 and 4 in central and Southern parts of the basin. The maximum value of B_s is obtained in subcatchment 49 in Southern part of the basin and the minimum value of V_f is obtained in subcatchment 44 in Southern part of the study area.

The base of the most recent structures of the Alborz mountain range was a Pleistocene uplifting phase that formed some large thrust faults such as Mosha, Taleghan, Emamzadeh Davud and Purkan-Vadij faults (Dedual, 1967). The Mosha fault with at least 4 km displacement (Allenbach, 1966) is the youngest feature in the area that across other structures. A tight compression in the Central Alborz with fold axis trending NW-SE also produced during the Late Pliocene phase (Gansser and Huber, 1962). The main folds in the study area are the Kahar anticline, Kuhe-Morud, Varishsangan Anticline and the Arangeh Syncline (Gansser and Huber, 1962).

The morphometric analysis described above allows us to interpret the tilting of the Karaj River and its tributaries based on their positions and flow direction respect to the tectonic structures of the study area. Based on tilting pattern in Fig. 11 three different areas were distinguished: (1) a Northern area, equivalent to the region with Paleozoic-Mesozoic bedrock, extends from Gachsar to Doab valley (Fig. 1, 11) with T values ranged from 0.02 to 0.25 (T average = 0.08) and migration direction of the Karaj River toward W-NW, (2) a central area from Doab to Asara with Tertiary bedrock and a little tilting (T average = 0.04) and (3) a southern area from Asara to Bailaghan with T-vectors generally show a main W-NW direction. T-values in this part ranged from 0.01 to 0.61 and the mean was 0.3. The major tributaries tilted to different directions depend on their flow directions respect to the structures; the rivers parallel to the structures have NE T-vectors, while the rivers perpendicular to the structures display W-NW T-vectors. Frequency diagram of asymmetry vectors is shown in Fig. 12. Mean vector magnitude for the Karaj River and its tributaries parallel to the structures was 0.1 (T-values),

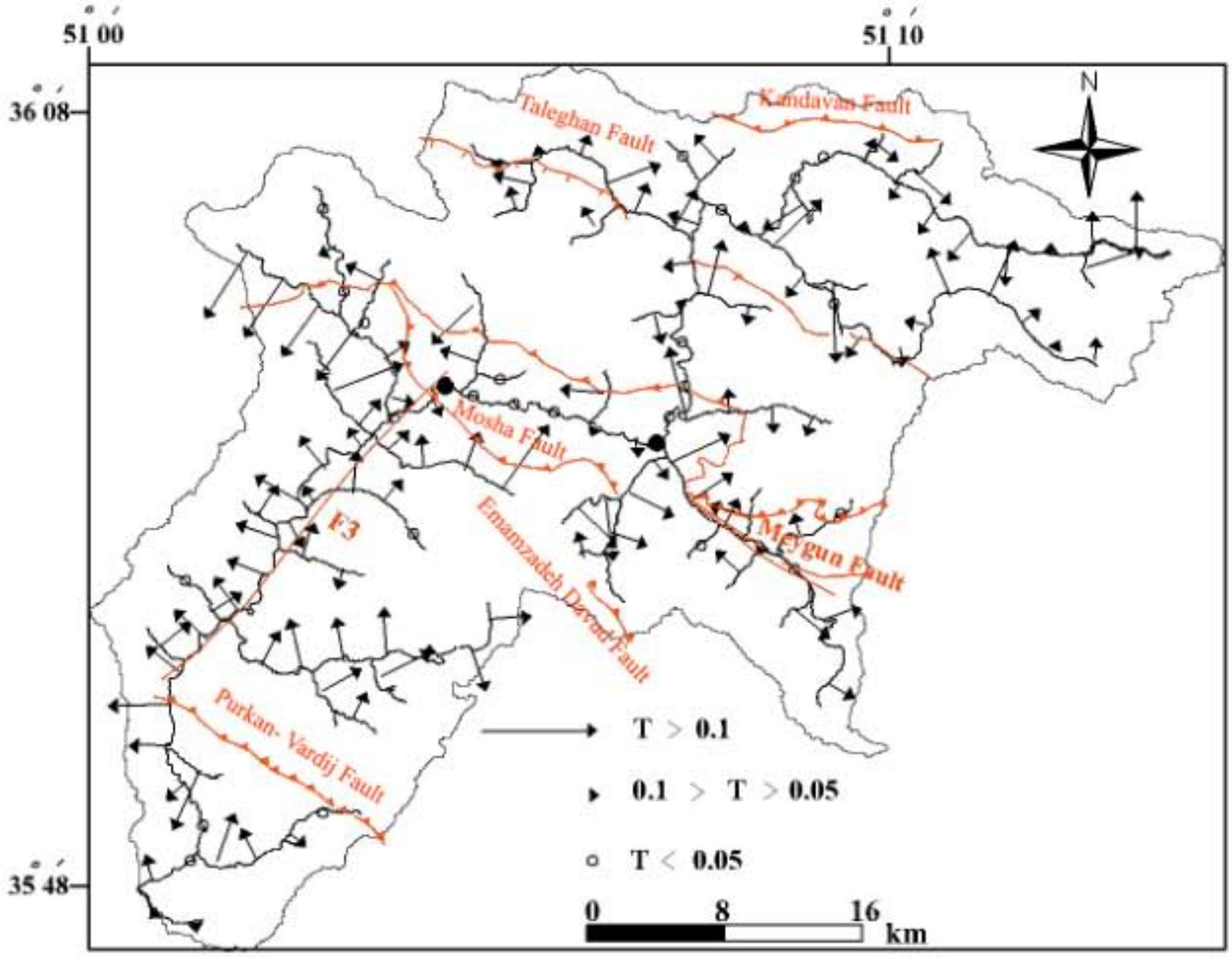

Fig. 11: Basin asymmetry vectors for the Karaj River and tributaries in the Karaj drainage basin. Length of the vectors denotes magnitude. Solid circles indicate boundaries of the three areas distinguished

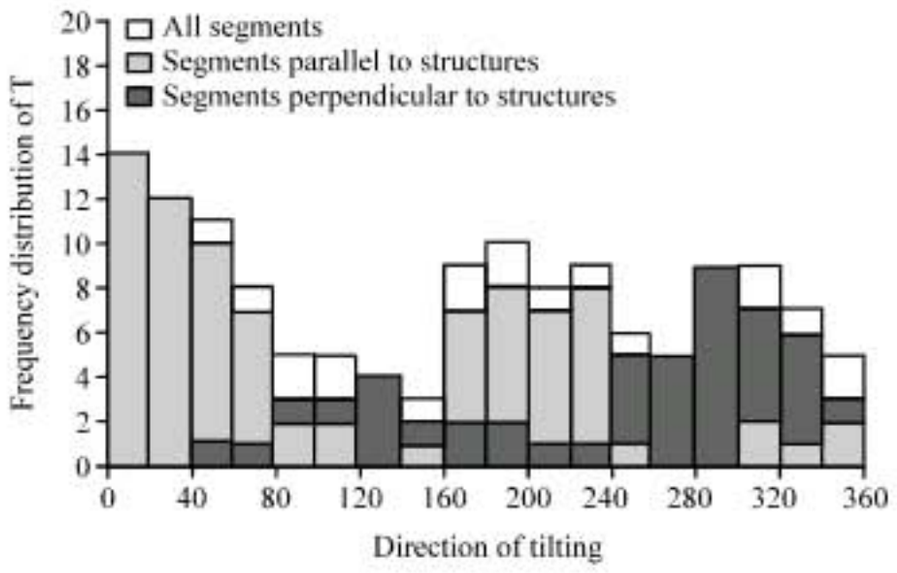

Fig. 12: Frequency diagram of asymmetry vectors in the Karaj drainage basin

39° (bearing), while in the North and South parts of the Karaj River and tributaries parallel to these parts, mean vector was 0.1 (T-values), 288° (bearing) (Fig. 13).

Before crossing the Mosha fault the Karaj River flows southward, while afterwards, it's flow direction changes toward West, parallel to the strike of Mosha fault, until the channel crossed the nose of the Kuhe-Morud, then taking a southerly path to the Karaj alluvial fan (Fig. 7).

Tilting of the Karaj River along it's channel is different in value and direction; in the North part of the basin the Hasanakdar fault with NW strike and SW dip direction has caused the migration of the Karaj River to the W-NW (section B-B´ in the Fig. 4), in the central part of the basin, the Karaj River flows parallel to the North flank of the Kuhe-Morud and its tilting is low (section C-C´ in Fig. 4). Finally, in the South part of the basin, the Karaj River has a maximum value of migration to W-NW (Table 1, Fig. 11). The high values of the AF occur in the most of the subcatchments in this part of the basin as well as the B_s index.

A NE-SW trending basement lineation F1 is in the southern part of the Karaj drainage basin along the Karaj River. Siah-sang mountain in the Northwestern block of this fault has a maximum elevation of 3378 m, but the Southeastern block of the fault contains mountain peak up to 3957 in Tuchal (Fig. 1). The average elevation of the Northwestern and Southeastern blocks is about 2334 and 2833 m, respectively. Although, there is the same lithology in both sides of the fault (Fig. 1), the Southeastern block has a more mean elevation than the Northwestern block. On the basis of geological map and

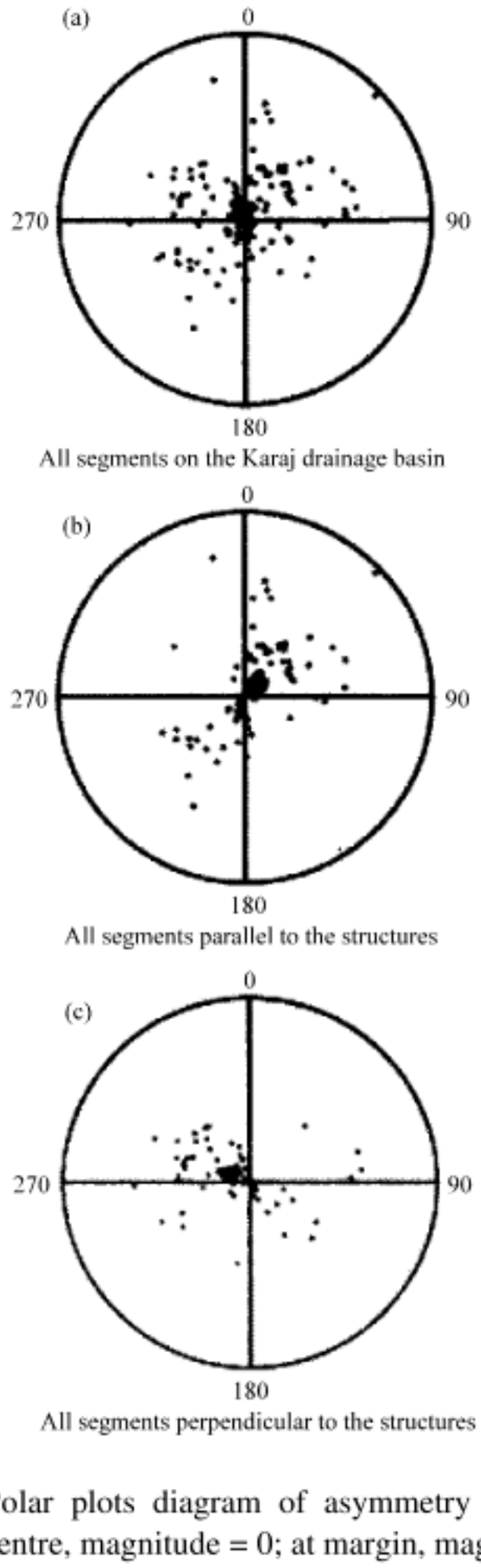

Fig. 13: Polar plots diagram of asymmetry vectors, at centre, magnitude = 0; at margin, magnitude = 1. Triangles indicate the mean vector for all data (a) Vector plotted = 137, Mean vector: T = 0.07, Bearing = 359, (b) vector plotted = 81, Mean vector: T = 0.1, Bearing = 39 and (c) vector plotted = 56, Mean vector: T = 0.07, Bearing = 288

field survey Mosha fault and two other longitudinal thrust faults (Emamzadeh Davud and Purkan-Vardij faults) in the southeastern block is considered to be causes of more uplifting and shortening here. So, it seems reasonable for the amount of shortening that basement lineation F_l can account. This is a place that Amir Kabir Dam was established and nevertheless there is very high resistance lithology, hard plutonic rocks, the maximum magnitude of tilting as an parameter of tectonic activity was obtained there. Because uplift is associated with incision, low values of V_f occur here.

CONCLUSION

Tilting direction has changed along the karaj River by differentiation of neotectonic activity of the south Central Alborz. The data are consistent with a NW tilting where the orientations of folds and fault blocks are perpendicular to the rivers, but where the structures oriented in the parallel directions to the rivers, tilting orientation is NE. The transverse topographic symmetry factor method shows a NW migration of all streams in the South termination of the Karaj River. The NW migration has caused of the more uplifting of SE part of the Karaj River that controlled by major thrusts. No relationship is found between the bedrock trends and the directions of stream migration and climate does not appear to be a plausible for drainage asymmetry. On the contrary, tectonics seems to explain the stream migration reasonably.

ACKNOWLEDGMENT

The authors would like to thank the Geological Survey of Iran for data supporting this research.

REFERENCES

Alexander, J. and M.R. Leeder, 1990. Geomorphology and surface tilting in an active extensional basin: SW Montana, USA. J. Geol. Soc. London, 147: 461-467.

Allen, M.B., M.R. Ghassemi, M. Shahrabi and M. Qorashi, 2003. Accommodation of late *Cenozoic oblique* shortening in the Alborz range, Northern Iran. J. Struct. Geol., 25: 659-672.

Allenbach, P., 1966. Geologie und petrographie des damavand und seiner Umgebung (Zentral Elburz), Iran. Mitteilungen aus dem Geologischen Institute der Eidgenoessischen Technischen Hochschule und der Universitaet Zurich, Neue Folge. pp: 63-144. http://e-collection.ethbib.ethz.ch/view/eth:32572

Barry, Y.C.C., W.S. Chen, L.C. Wu and C.W. Lin, 2007. Deformation front delineated by drainage pattern analysis and vertical movement rates, Southwestern Coastal Plain of Taiwan. J. Asian Earth Sci., 31: 251-264.

Berberian, M. and R.S. Yeatz, 2001. Contribution of archeological data to studies of earthquake history in the Iranian Plateau. J. Struct. Geol., 23: 563-584.

Bull, W.B. and L.D. McFadden, 1977. Tectonic geomorphology north and south of the *Garlock fault*. U.S. Geological Survey, California.

Burbank, D.W. and R.S. Anderson, 2001. Tectonic Geomorphology. Blackweel Science, Massachusetts, IBSN-10: 0632043865.

Cox, R.T., 1994. Analysis of drainage-basin symmetry as a rapid technique to identify areas of possible quaternary tilt-block tectonics: An example from the Mississippi Embayment. Geol. Soc. Am. Bull., 106: 571-581.

Dedual, E., 1967. Zur geologie des mittleren und unteren karaj-tales, zentral-elburz (Iran). Mitteilungen aus dem Geologischen Institute der Eidgenoessischen Technischen Hochschule und der Universitaet Zurich, Zürich, SUISSE (Université de soutenance), Neue Folge pp: 76-123. INIST-CNRS, Cote INIST: TM 936.

Ehteshami, M.M. and A. Yassaghi, 2006. Geometry and kinematics of the *Mosha fault*, South central Alborz Range, Iran: An example of basement involved thrusting. J. Asian Earth Sci., 29: 928-938.

El-Hamdouni, R., C. Irigaray, T. Fernandez, J. Chacon and E.A. Keller, 2008. Assessment of relative active tectonics, Southwest border of the Sierra Nevada (Southern Spain). Geomorphology, 96: 150-173.

Emami, M.H., 1993. Geological map of Tehran quadrangle scale 1:100,000. Geological Survey of Iran.

Gansser, A. and H. Huber, 1962. Geological observations in the central Alborz, Iran. Schweizerische Mineralogische und Petrographische Mitteilungen, 42: 583-630.

Hayakawa, Y. and T. Oguchi, 2006. DEM-based identification of fluvial knickzones and its application to Japanese mountain rivers. Geomorphology, 78: 90-106.

Keller, E.A. and N. Pinter, 2002. Active Tectonics, Earthquakes, Uplift and Landscape. 2nd Edn., Prentice Hall Earth Sciences Series, USA., ISBN: 0130882305, pp: 362.

Nazari, H., J.F. Ritz, R. Salamati, A. Shafei and A. Ghassemi, 2009. Morphological and palaeoseismological analysis along the *Taleghan fault* (Central Alborz, Iran). Geophys. J. Int., 178: 1028-1041.

Ramírez-Herrera, M.A., 1998. Geomorphic assessment of active tectonics in the Acambay Graben, Mexican volcanic belt. Earth Surface Process. Landforms, 23: 317-332.

Reinfelds, I., T. Cohen, P. Batten and G. Brierley, 2004. Assessment of downstream trends in channel gradient, total and specific stream power: A GIS approach. Geomorphology, 60: 403-416.

Ritz, J.F., H. Nazari, A. Ghassemi, R. Salamati, A. Shafei, S. Solaymani and P. Vernant, 2006. Active transtension inside Central Alborz: A new insight into Northern Iran-Southern *Caspian geodynamics*. Geol. Soc. Am., 34: 477-480.

Salvany, J.M., 2004. Tilting neotectonics of the Guadiamar drainage basin, SW Spain. Earth Surface Process. Landforms, 29: 145-160.

Schumm, S.A., J.F. Dumont and J.M. Holbrook, 2000. Active Tectonics and Alluvial Rivers. Cambridge University Press, Cambridge, New York, USA., ISBN: 0-521-66110-2, pp: 276.

Silva, P.G., J.L. Goy, C. Zazo and T. Bardajm, 2003. Fault generated mountain fronts in Southeast Spain: Geomorphologic assessment of tectonic and earthquake activity. Geomorphology, 50: 203-225.

Vahdati-Daneshmand, F., 2001. Geological map of marzan abad quadrangle scale 1:100,000. Geological Survey of Iran.